A high-temperature Raman scattering study of the phase transitions in $GaPO_4$ and in the $AlPO_4$–$GaPO_4$ system

2006 J. Phys.: Condens. Matter 18 4315

(http://iopscience.iop.org/0953-8984/18/17/018)

INSTITUTE OF PHYSICS PUBLISHING JOURNAL OF PHYSICS: CONDENSED MATTER

J. Phys.: Condens. Matter **18** (2006) 4315–4327 doi:10.1088/0953-8984/18/17/018

A high-temperature Raman scattering study of the phase transitions in $GaPO_4$ and in the $AlPO_4$–$GaPO_4$ system

E Angot[1,2], R Le Parc[1], C Levelut[1], M Beaurain[2], P Armand[2], O Cambon[2] and J Haines[2]

[1] Laboratoire des Colloïdes, des Verres et des Nanomatériaux, UMR CNRS 5587, Université Montpellier II, cc026, Place E Bataillon, F-34095 Montpellier Cedex 5, France
[2] Laboratoire de Physicochimie de la Matière Condensée, UMR CNRS 5617, Université Montpellier II, cc003, Place E Bataillon, F-34095 Montpellier Cedex 5, France

E-mail: jhaines@lpmc.univ-montp2.fr

Received 3 February 2006, in final form 24 March 2006
Published 13 April 2006
Online at stacks.iop.org/JPhysCM/18/4315

Abstract

$Al_{1-x}Ga_xPO_4$ solid solutions ($x = 0.2$, 0.3, 0.38, 0.7) and the pure $AlPO_4$ ($x = 0$) and $GaPO_4$ ($x = 1$) end members with the α-quartz-type structure were studied by Raman scattering. An investigation as a function of composition enabled the various modes to be assigned, in particular coupled and decoupled vibrations. The tetrahedral tilting modes, which have been linked to high-temperature phase transitions to β-quartz-type forms, were found to be decoupled. In addition, it is shown that Raman spectroscopy is a powerful technique for determining the gallium content of these solid solutions. Single crystals with $x = 0.2$, 0.38, and 1.0 ($GaPO_4$) were investigated at high temperature. The composition $Al_{0.8}Ga_{0.2}PO_4$ was found to exhibit sequential transitions upon heating to the β-quartz and β-cristobalite forms at close to 993 K and 1073 K, respectively. Direct α-quartz–β-cristobalite transitions were observed for the two other compositions at close to 1083 K and 1253 K, respectively, upon heating. The spectra of the β-quartz and β-cristobalite forms indicate the presence of significant disorder. Back transformation to the α-quartz-type form occurred readily with a hysteresis of less than 100 K for the composition $x = 0.38$ and for pure $GaPO_4$. Rapid cooling was necessary to obtain the metastable α-cristobalite form. In contrast, for $Al_{0.80}Ga_{0.20}PO_4$, the α-cristobalite form was obtained even upon slow cooling.

1. Introduction

Phase stability in silica is of great importance for earth and materials science, crystal chemistry and solid state physics. The study of analogue materials (GeO_2, BeF_2, PON and ABO_4, where A = B, Al, Ga, Fe; B = P, As) provides models for SiO_2 and new materials with potentially improved properties for various technological applications (glass, vitroceramics and, in the case

of the α-quartz-type form, piezoelectric resonators). The stable form of silica under ambient conditions is trigonal α-quartz. Transitions are observed at high temperature to hexagonal β-quartz, HP(hexagonal primitive)-tridymite and, finally, cubic β-cristobalite [1]. These high-temperature forms are characterized by significant dynamic disorder linked to excited rigid-unit modes [2–4]. Some degree of disorder is also observed in α-quartz at high temperature prior to the α–β transition [4, 5]. Disorder has also been observed by Raman spectroscopy for $AlPO_4$ [6] and by total neutron scattering for $GaPO_4$ [7]. These results indicate that disorder plays a major role in the high-temperature behaviour of these materials. Disorder will also have an important impact on the piezoelectric properties of the α-quartz-type form [5, 7].

Structure-property relationships have been developed for α-quartz homeotypes, linking the thermal stability of the α-quartz-type phase and a number of physical, dielectric and piezoelectric properties to the structural distortion with respect to the β-quartz structure type [8–18]. This distortion can be described by the intertetrahedral bridging angle and the tetrahedral tilt angle. The latter has also been taken as the order parameter for the α–β transition in quartz [19]. 'Soft-mode behaviour' [20–25] has also been related to tetrahedral tilting in these materials; however, recent results indicate that the phase transition mechanism is more complex and that disorder is involved [4–6]. The α–β phase transition is not observed for the more distorted materials such as $GaPO_4$, which undergoes a direct transition to the β-cristobalite form at 1206 K [26]. This reconstructive phase transition is associated with slow kinetics and, depending on the starting material and the thermal treatment, differences in transition temperatures and the reversibility of the transition have been observed [26–29]. In many cases, the β-cristobalite form was found to transform to the α-cristobalite-type phase upon cooling [7, 26–29].

Several solid solutions exist among α-quartz homeotypes (SiO_2–GeO_2 [30–32], SiO_2–PON [11], SiO_2–$AlPO_4$ [33], $AlPO_4$–$GaPO_4$ [34–39], $AlPO_4$–$AlAsO_4$ [34], and $AlPO_4$–$FePO_4$ [40]). In the $Al_{1-x}Ga_xPO_4$ system [38], the structural distortion varies in an essentially linear way as a function of x, which may open a way to tune the piezoelectric properties of crystals in this system by varying the composition. High-temperature x-ray diffraction results [39] indicate that the stability of the α-quartz form increases as a function of x and that the β-quartz form is found only to exist as a stable phase for $x < 0.3$. Above this value, the direct transition to the β-cristobalite form was observed. The transition kinetics were found to be very slow.

The Raman spectra of $AlPO_4$ and $GaPO_4$ have been described in detail [6, 24, 25, 41–44]. Intensive study of the Raman spectra of quartz and cristobalite forms of $AlPO_4$ at high temperature has also been reported [6, 24, 25, 45]. High-temperature Raman data for $GaPO_4$ are limited to studies [42, 46] up to 973 K, which is well below the α-quartz–β-cristobalite phase transition temperature (1206 K). Raman data for $Al_{1-x}Ga_xPO_4$ mixed crystals are available only for $x = 0.1$ at room temperature [36].

In the present study, the Raman spectra of $Al_{1-x}Ga_xPO_4$ materials were investigated as a function of x in order to assign the vibrational modes. Selected compositions were then investigated at high temperature in order to improve our understanding of the phase transition sequence in these materials, their reversibility and kinetics. The high-temperature Raman spectra also provide information on disorder in these materials at high temperature. These results have important implications for the use of these materials in piezoelectric devices.

2. Experimental section

2.1. Synthesis of $GaPO_4$ and $Al_{1-x}Ga_xPO_4$ single crystals and powders

Crystal growth of $GaPO_4$ was carried out in air in a single temperature zone, SiC resistance heater furnace [47–49]. Different amounts (wt%) of the $Li_2Mo_3O_{10}$ or $K_2Mo_3O_{10}$ flux

were mixed with the α-$GaPO_4$ powder, which had been prepared by dissolving metallic Ga (>99.999%) in nitric acid followed by precipitation with phosphoric acid. The $GaPO_4$-flux mixture was heated from room temperature to 1223 K. $GaPO_4$ single crystals were grown in a direct solubility range between 1223 K and 873 K. After cooling, millimetric single crystals were separated from the growth solution by dissolving the residual flux in warm water.

The $Al_{1-x}Ga_xPO_4$ single crystal and powder samples were prepared by hydrothermal methods [34, 38, 39]. Suitable quantities of solutions of $AlPO_4$ and $GaPO_4$ in sulfuric acid were mixed, taking into account differences in solubility, placed in a PTFE-lined autoclave, and heated in order to induce crystallization. The composition of the single crystals was measured by electron microprobe analysis [34, 38]. The composition of the powder samples was based on the c/a cell parameter ratio obtained from x-ray powder diffraction measurements performed on a PANanalytical X'Pert diffractometer equipped with an X'Celerator detector using Ni-filtered, Cu Kα radiation [39].

2.2. High-temperature Raman scattering

Raman spectra of the above materials and commercial $AlPO_4$ were obtained using an argon ion laser (514.532 nm) with a Jobin-Yvon T64000 triple monochromator equipped with an Olympus microscope and a CCD cooled to 140 K. The sample was placed on a small platinum block in the oven of a Linkam TS 1500 heating stage under the microscope. A 50× objective was used to investigate sample regions with a diameter of about 3 μm. The laser powers at the sample were 8–12 mW. The temperature was measured using a thermocouple, and was checked from the ratio of Stokes and anti-Stokes intensities according to the Bose population factor ($n(\tilde{\nu}, T)$).

3. Results and discussion

3.1. Composition dependence of the Raman spectrum of $Al_{1-x}Ga_xPO_4$

Group theory predicts that the pure end members of α-quartz-type $AlPO_4$ and $GaPO_4$ (trigonal $P3_121$ D_3^4, $Z = 3$) will exhibit 54 modes of vibration:

$$\Gamma = 8A_1 + 10A_2 + 18E$$

of which $1A_2 + 1E$ are acoustic modes.

The remaining optical modes are:

$$\Gamma = 8A_1 + 9A_2 + 17E.$$

There are 25 modes that are predicted to be Raman active (8 non-degenerate A_1 + 17 doubly degenerate E). This compares to the 12 modes predicted for α-quartz (SiO_2). The unit cell is doubled in the case of the phosphates due to the ordering of the two distinct cations along the **c** direction. The situation is more complicated for the $Al_{1-x}Ga_xPO_4$ solid solutions. There is no evidence for Al/Ga ordering in this system. The observed modes involving Al and/or Ga may be coupled, leading to one mode, or decoupled, yielding distinct modes involving Al or Ga.

Raman spectra on single crystals or powders were obtained for a series of compositions (figure 1, table 1). It can be seen that two types of modes are present. There are modes that vary continuously in frequency as a function of composition between the two end members due to the difference in mass between Al and Ga (coupled modes) and other modes that are linked to either AlO_4 or GaO_4 tetrahedra and do not appear in the spectrum of the opposite end member (decoupled modes italics in table 1). The coupled modes correspond to vibrations principally involving internal stretching (∼1050–1250 cm^{-1}) and bending (∼400–500 cm^{-1}) of the PO_4

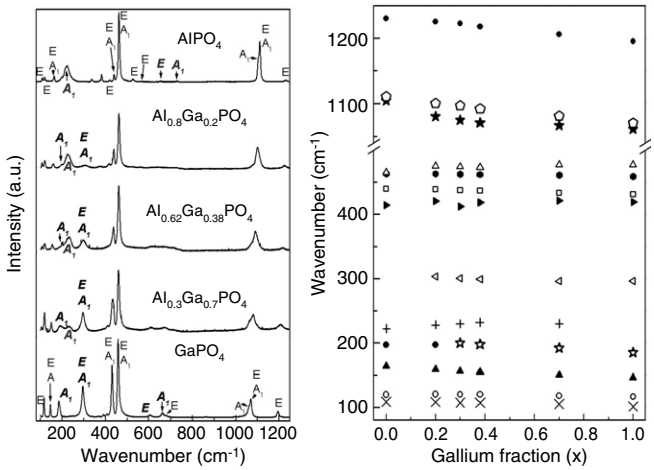

Figure 1. Raman spectra (left) and wavenumber of the Raman modes (right) of $Al_{1-x}Ga_xPO_4$ as a function of composition.

tetrahedra and lattice modes (below ∼180 cm^{-1}), whereas the decoupled modes correspond to those involving Al/Ga vibrations (∼500–800 cm^{-1}) and libration (∼180–300 cm^{-1}) of the AlO_4 or GaO_4 tetrahedra. The coupling is weak for certain internal modes such as bending of the PO_4 tetrahedra, indicating that they are localised. The difference in behaviour between the two types of modes is related to the substitution, which is restricted to the *A*-site (Al/Ga) in the structure, and to the different environment around each type of tetrahedron. Each AlO_4 or GaO_4 tetrahedron is linked to four PO_4 units; there are thus no direct links between AlO_4 or GaO_4 units, which are always separated by a PO_4 unit. In contrast, each PO_4 tetrahedron is linked to four $(Al/Ga)O_4$ units, with the average number of neighbouring Al- or Ga-centred tetrahedra depending on the composition of the solid solution. Coupling may thus occur between vibrations involving neighbouring PO_4 and $(Al/Ga)O_4$ tetrahedra, but is not very efficient between the more distant AlO_4 or GaO_4 units. It is particularly interesting to note that the librational modes of the AlO_4 or GaO_4 tetrahedra at 222 cm^{-1} and 296 cm^{-1}, which have been linked to soft-mode or incipient soft-mode behaviour [24, 46], are decoupled and thus do not provide an explanation for the observed slope of the phase boundary between the α- and β-quartz-type forms [34, 37, 39].

Certain coupled modes exhibit large shifts as a function of composition. This is particularly the case for the mode at 1111 cm^{-1} in $AlPO_4$, which is primarily dominated by P–O stretching. The shift of this mode as a function of composition can be expressed using the following second-order polynomial fit:

$$\tilde{\nu}\ (\mathrm{cm}^{-1}) = 1110.84 - 50.59x + 10.71x^2.$$

The available spectral resolution allows the composition to be rapidly determined with an accuracy of ±1%. This technique provides a quick alternative to electron microprobe analysis or x-ray diffraction using Vegard's law, which are more time consuming (sample preparation, acquisition time, and data analysis).

3.2. Temperature dependence of the Raman spectrum of $Al_{1-x}Ga_xPO_4$

Three selected compositions with respect to their phase transition behaviour were studied at high temperature: $Al_{0.80}Ga_{0.20}PO_4$, $Al_{0.62}Ga_{0.38}PO_4$ and pure $GaPO_4$.

Table 1. Raman modes (cm^{-1}) of α-quartz-type $Al_{1-x}Ga_xPO_4$ as a function of composition. Mode assignments are based on single-crystal Raman studies [6, 36, 41, 43]. (Note: decoupled modes in italics; *vw* = very weak).

Mode [6, 36, 41, 43]	$x = 0$	$x = 0.2$	$x = 0.3$	$x = 0.38$	$x = 0.7$	$x = 1$
E	109	107	107	107	105	101
E	120	120	120	120	118	116
E, A_1	164	158	156	155	150	146
E	197	197	vw	vw	vw	191
A_1	—	—	*199*	*198*	*191*	*185*
A_1	*222*	*228*	*229*	*232*	*229*	—
E, A_1	—	*301*	*300*	*299*	*296*	*296*
E	419	417	421	418	412	414
E, A_1	439	438	437	436	433	431
E, A_1	463	463	462	462	461	459
E	526	—	—	—	—	—
E	*567*	—	—	—	—	—
E	—	*vw*	*vw*	*614*	*610*	*603*
E	*654*	*vw*	*vw*	*vw*	*vw*	—
A_1	—	*vw*	*vw*	*vw*	*vw*	*661*
E	700	vw	vw	vw	672	676
A_1	*728*	*vw*	*vw*	*vw*	*714*	—
E	*751*	*vw*	*vw*	*vw*	*741*	—
A_1	1103	1074	1075	1071	1066	1061
E, A_1	1111	1101	1096	1092	1081	1070
E	1230	1226	1222	1218	1206	1195

3.2.1. $GaPO_4$. Gradual broadening and shifts in frequency of the Raman peaks of flux-grown single crystals of α-quartz-type $GaPO_4$ occur over the wide temperature range of stability of the α-quartz-type form up to 1253 K (figures 2 and 3). These changes both occur in a continuous manner and no marked tendency towards a β-quartz form was observed. The mode at 296 cm^{-1} associated with the libration of the GaO_4 tetrahedra in particular shifts to 269 cm^{-1} over the temperature interval between 295 K and 1233 K, and the line width increases continuously (figure 4). Transitions to β-quartz forms are linked in particular to tetrahedral tilting. This mode, however, does not exhibit any marked instability.

Instead of a transition to a β-quartz form, a reconstructive phase transformation to the β-cristobalite form has been observed [7, 26–29]. In the present study, the temperature was slowly increased up to 1253 K. At this temperature, this first-order transformation was found to occur gradually within 1 h (figure 5). The single crystal was found to transform to polycrystalline material at this phase transition. The sample was further heated up to 1353 K. The spectrum of the highly disordered β-cristobalite phase is characterised by a series of broad bands and by the disappearance of the low-frequency modes. Group theory for an average $F\bar{4}3m$ (T_d^2, $Z = 4$) structure with Ga, P and O on 4a (0, 0, 0), 4c (1/4, 1/4, 1/4) and 16e (x, x, x) sites, respectively, yields the following result:

$$\Gamma = A_1 + E + T_1 + 4T_2$$

of which the $1T_2$ mode is acoustic.

Five modes ($A_1 + E$ (doubly degenerate) $+ 3T_2$ (triply degenerate)) are Raman active. The present results (table 2), in which at least 8 modes are observed, indicate that the average high-symmetry structure is unable to explain the observed Raman spectrum. The observation of at least three additional modes indicates that the local symmetry is lower in the instantaneous

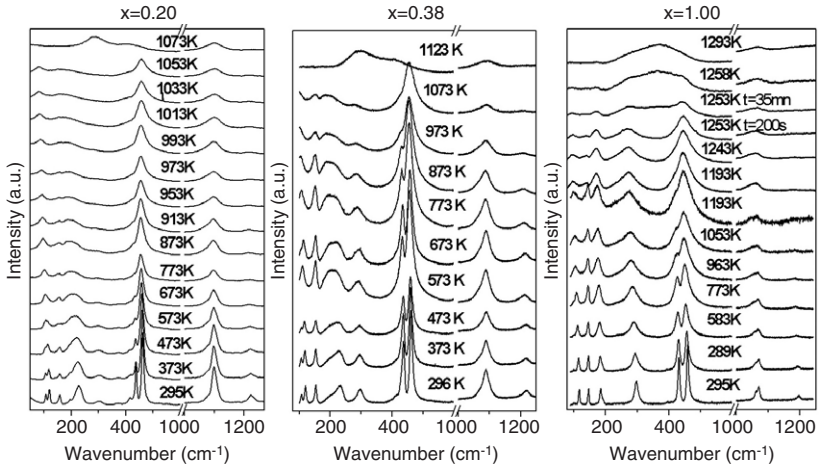

Figure 2. Raman spectra of $Al_{1-x}Ga_xPO_4$ ($x = 0.20, 0.38, 1.00$) on heating.

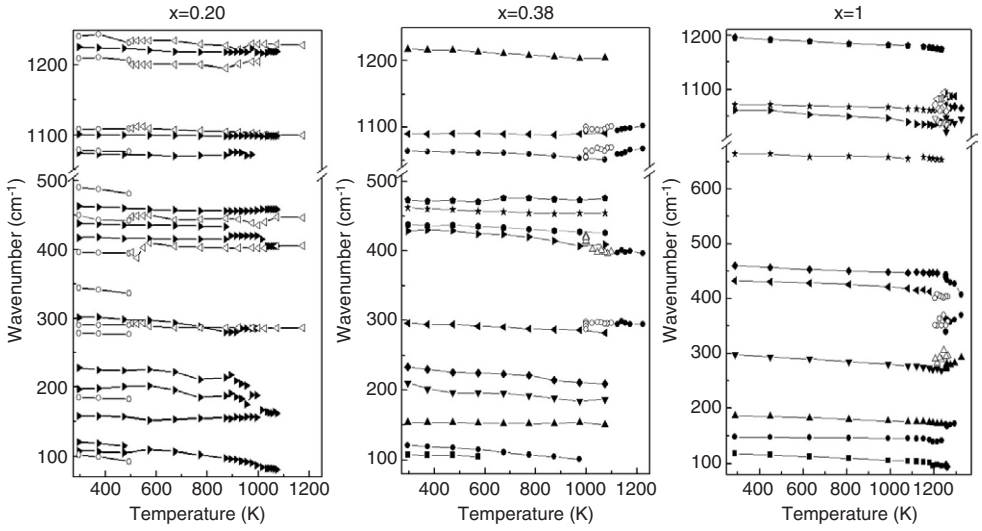

Figure 3. Temperature dependence of the principal Raman modes of $Al_{1-x}Ga_xPO_4$ ($x = 0.20$, 0.38, 1.00). Solid symbols correspond to heating runs. Open symbols correspond to cooling runs.

structure on the Raman timescale. Such a reduction in symmetry can be linked to dynamic disorder, which has been identified in recent total neutron scattering results on the β-cristobalite form of $GaPO_4$ [7]. The latter indicate that the oxygen atoms do not occupy the 16e sites, but are distributed in a disordered way on lower-symmetry 96i sites along a ring perpendicular to the Ga–P vector, which yields reasonable values for the Ga–O and P–O bond distances and Ga–O–P bond angles. This angle would have an unrealistic value of 180° in the ordered structure. Locally, in the instantaneous structure, the bond angle is typically of the order of 139°, producing a lower-symmetry configuration [7].

The reverse transformation to the α-quartz form was found to occur readily at 1193 K. Complete reversibility of this transition has been observed previously [26, 27]. However, in a large number of cases, depending on the method of synthesis and the cooling rate, only partial

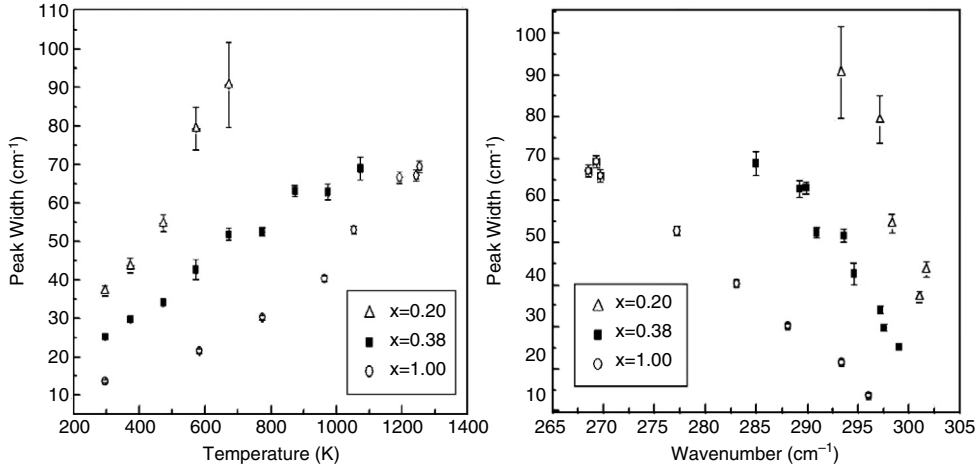

Figure 4. Temperature (left) and wavenumber (right) dependence of the line width of the GaO_4 librational modes of $Al_{1-x}Ga_xPO_4$ ($x = 0.20, 0.38, 1.00$).

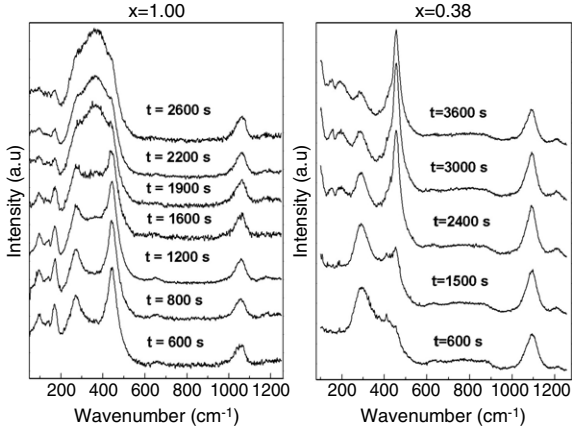

Figure 5. Evolution of the Raman spectra of $GaPO_4$ at 1253 K (heating cycle—left) and $Al_{0.62}Ga_{0.38}PO_4$ at 998 K (cooling cycle—right).

retransformation to the α-quartz form has been observed, with a quantity of the β-cristobalite form being retained to much lower temperatures and finally undergoing a displacive phase transition near 853 K to the α-cristobalite form [7, 26–29]. In many cases, the recovered material thus corresponds to a mixture of the α-quartz form and the α-cristobalite form or even the latter pure. In the present flux-grown samples, without significant hydroxyl group impurities [47–49], the reverse transition occurs readily. In contrast, in materials prepared by hydrothermal methods, defects linked to OH groups may stabilise the disordered β-cristobalite form. In all cases, a high cooling rate ($\sim$100 K min^{-1}) also favours the metastable retention of the β-cristobalite form below the thermodynamic phase transition temperature of 1206 K. In many studies, principally on samples prepared by hydrothermal methods, cooling rates of the order of only 5–10 K min^{-1} were needed to retain the β-cristobalite form [28, 29]. In the present study, a series of different cooling rates was used, starting from an initial temperature of 1473 K. A cooling rate of 100 K min^{-1} was needed in order to retain the β-cristobalite form and

Table 2. Raman modes (cm^{-1}) of the α- and β-cristobalite-type forms of $Al_{1-x}Ga_xPO_4$. (Note: ho = possible higher-order modes (note the strong increase in the intensities of these modes at high temperature, figure 6)).

Mode assignment	$x = 0$ [45]		$x = 0.2$		$x = 0.38$		$x = 1$	
in the α phase [44, 45]	α (296 K)	β (547 K)	α (293 K)	β (503 K)	α (296 K)	β (1123 K)	α (843 K)	β (853 K)
A	99		102		104		90	90
B_2, B_3	145	143						
A	188		185	175	173	176	148	150
B_2, B_3	279	270	290, 278	293	273	295	245	220
B_2, B_3 or A			344		348		343	300
A	388				387		388	390
A		402	396	396	403	400		
		450	450	448				
A, B_2, B_3	482		530, 490	522	496	498	490	
B_2, B_3			629	634	629	633	619	635
B_2, B_3			645		644			
B_2, B_3	713		708		686			
A, ho			720	736	727	762	750	733
ho						870	860	833
B_1	924	920	905	920				
A	996	995						
B_2, B_3	1013	1017		990				
							1013	
			1078	1073	1079	1066	1066	1066
B_2, B_3	1113	1110	1108	1110	1096	1097		
A	1124	1125	1108		1109			
A			1209	1201	1199	1214	1180	1193
			1241	1235				

to subsequently observe the β-cristobalite-type–α-cristobalite-type phase transition at close to 853 K. This phase transition is associated (figure 6) with the sharpening of the Raman modes observed at 843 K corresponding to the formation of an ordered phase. The predictions of group theory for an α-cristobalite-type form (space group $C222_1$, D_2^5, $Z = 4$) are the following:

$$\Gamma = 8A_1 + 10B_1 + 9B_2 + 9B_3$$

of which $1B_1 + 1B_2 + 1B_3$ are acoustic modes.

All 33 remaining modes are Raman active. At least 9 modes were observed in the Raman spectrum at 843 K (table 2). The sample was heterogeneous. Whereas no Raman peaks from the quartz-type phase could be detected in the grain studied (figure 6), other grains contained various quantities of the α-quartz-type form. The Raman spectrum of the α-cristobalite-type form was studied down to 373 K; however, only the α-quartz-type form could be identified in the spectrum at ambient temperature.

3.2.2. $Al_{0.62}Ga_{0.38}PO_4$. Globally, the high-temperature behaviour of $Al_{0.62}Ga_{0.38}PO_4$ is similar to that of pure $GaPO_4$, but with lower phase transition temperatures due to the substitution of Ga by Al, in agreement with previously determined phase diagrams [34, 37, 39]. As in $GaPO_4$, gradual broadening of the Raman bands are observed and no evidence of any pronounced instability is present (figures 2–4). The transition to the β-cristobalite form occurs rapidly above 1080 K. At least eight Raman modes were observed in this phase, as

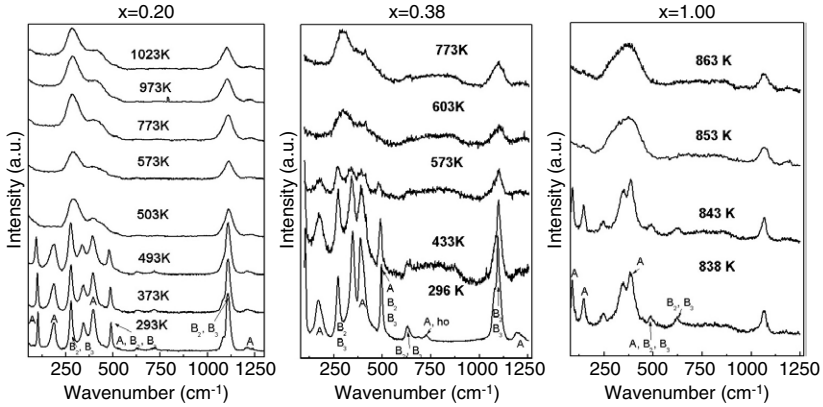

Figure 6. Raman spectra of the cristobalite-type forms of $Al_{1-x}Ga_xPO_4$ ($x = 0.20, 0.38, 1.00$) on cooling.

in the corresponding phase of $GaPO_4$ (table 2). Upon slow cooling, the reverse transition to the α-quartz-type form was observed. This process required about 1 h at 998 K (figure 5). This material, synthesized under hydrothermal conditions in sulphuric acid, has a lower content of hydroxyl groups than hydrothermally prepared $GaPO_4$ in phosphoric acid due to the dehydrating properties of sulphuric acid. The observed slower kinetics with respect to $GaPO_4$ may thus be mainly due to the lower transition temperatures involved, rather than a consequence of the presence of hydroxyl groups, which may stabilise the β-cristobalite-type phase. In contrast, the β-cristobalite-type form was retained to much lower temperatures upon rapid cooling ($\sim$100 K min^{-1}) and the β-cristobalite-type–α-cristobalite-type phase transition was observed at close to 573 K (figure 6), in agreement with previous studies [34, 37, 50].

3.2.3. $Al_{0.80}Ga_{0.20}PO_4$. The peaks in the Raman spectra of the α-quartz-type form of $Al_{0.80}Ga_{0.20}PO_4$ broaden quite rapidly as a function of temperature (figure 2). This broadening becomes increasingly marked above 773 K. This effect is much more important than in $Al_{0.62}Ga_{0.38}PO_4$ and $GaPO_4$ and is similar to the behaviour observed for $AlPO_4$ [6]. In the present case, this damping can be seen particularly in the broadening of the decoupled GaO_4 tetrahedral libration (301 cm^{-1} at 295 K) (figure 4). The observed damping is similar to that observed for the ω_2 A_1 mode in $AlPO_4$ [6], indicating that the minority GaO_4 tetrahedra follow the major component AlO_4 tetrahedra. This damping can be related to increased instability in the structure, as the observed behaviour is distinct from that of $Al_{0.62}Ga_{0.38}PO_4$ and $GaPO_4$, for which no α-quartz–β-quartz transition is present. Dynamic disorder will contribute to this damping well below the α–β transition temperature. Total neutron scattering studies show that in quartz [4, 5], a material which undergoes an α–β transition, the disorder increases much faster as a function of temperature than in $GaPO_4$ [7], which does not exhibit a β-quartz phase. The contribution due to dynamic disorder is summed to anharmonic contributions, which induce a temperature dependence in the phonon lifetimes. In the present study, the damping increases from 37 cm^{-1} to 79 cm^{-1} between 300 K and 573 K, corresponding to a decrease in wavenumber from 301 cm^{-1} to 297 cm^{-1} (figure 4). A similar shift is observed for pure $GaPO_4$ over the same temperature range. This temperature dependence of a vibrational mode can be expressed as the sum of two contributions:

$$\left(\frac{\mathrm{d}\tilde{\nu}_i}{\mathrm{d}T}\right)_P = \left(\frac{\mathrm{d}\tilde{\nu}_i}{\mathrm{d}T}\right)_{\text{explicit}} + \left(\frac{\partial\tilde{\nu}_i}{\partial V}\right)_T \left(\frac{\mathrm{d}V}{\mathrm{d}T}\right)_P .$$

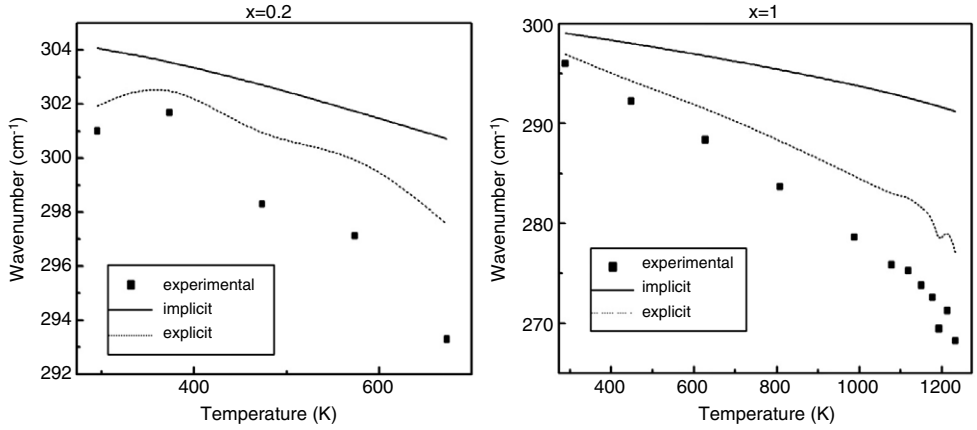

Figure 7. Implicit and explicit contributions to the temperature dependence of the wavenumber of the GaO_4 librational modes of $Al_{1-x}Ga_xPO_4$ ($x = 0.20, 1.00$).

The first is termed the explicit contribution (self-anharmonic term) and the second is termed the implicit contribution (thermal expansion term). The temperature shift of a mode due to the implicit contribution can be expressed as [43]:

$$\tilde{\nu}_i(T)_{\text{implicit}} = \tilde{\nu}_i(T=0)\left[\frac{V(T=0)}{V(T)}\right]^{\gamma_i}$$

where the quasi-harmonic mode Grüneisen parameter

$$\gamma_i = -\frac{V}{\tilde{\nu}_i}\left(\frac{\mathrm{d}\tilde{\nu}_i}{\mathrm{d}V}\right) = \frac{B_0}{\tilde{\nu}_i}\left(\frac{\partial\tilde{\nu}_i}{\partial P}\right)_T$$

and B_0 is the isothermal bulk modulus of the material. It has been shown that the self-anharmonic term dominates the frequency shift for the majority of modes, including this vibration, below room temperature in pure $GaPO_4$ [43]. In the present work, similar behaviour is observed at high temperature for both $GaPO_4$ and $Al_{0.80}Ga_{0.2}PO_4$, for the mode near 300 cm^{-1} (figure 7), assuming, as a first approximation, that γ_i is independent of temperature. The calculated implicit contributions were obtained using the low-temperature Raman data and the known γ_i value for this mode in $GaPO_4$ (0.65) [43] and the available thermal expansion results [51]. The explicit contribution was obtained by subtracting the implicit contribution from the experimental results. The situation is more difficult for $Al_{0.80}Ga_{0.2}PO_4$, as, although thermal expansion data are available [52], no low-temperature studies have been performed. The differences in volume and wavenumber between $GaPO_4$ and $Al_{0.80}Ga_{0.2}PO_4$ were thus assumed to be constant from 0 K to room temperature.

In the present study, the observed increase in damping is very large with respect to the decrease in wavenumber for $Al_{0.80}Ga_{0.2}PO_4$, whereas this is not the case for $GaPO_4$, in spite of the fact that the self-anharmonic contributions to the wavenumber shift are similar. This is an indication of an additional contribution to the line width due to disorder. The line width of this mode in $Al_{0.80}Ga_{0.2}PO_4$ increases to such an extent with further increases in temperature, with values of well over 100 cm^{-1}, that it becomes very difficult to measure the line width accurately above 700 K.

The vibrational bands become more symmetrical above 993 K, particularly in the region between 150 cm^{-1} and 200 cm^{-1} (figure 2). In addition, there is a reduction in the number of modes (figure 3 and table 3). This behaviour is very similar to $AlPO_4$ [6] at the α–β

Table 3. Raman modes (cm^{-1}) of the quartz-type forms of $Al_{0.8}Ga_{0.2}PO_4$. Mode assignments are based on the single-crystal Raman study of $Al_{0.9}Ga_{0.1}PO_4$ [36].

Mode in α phase [36]	α (300 K)	α (953 K)	β (1063 K)
E	107	92	82
E	120	—	—
E, A_1	158	157	164
E	197	202	—
A_1	228	—	—
E, A_1	301	285	283
E	417	—	—
E, A_1	438	420	405
E, A_1	463	456	458
A_1	1074	1072	1075
E, A_1	1101	1099	1098
E	1226	1218	1219

phase transition at which the distinct coupled AlO_4 A_1 modes ω_1 and ω_2 with a characteristic resonance dip are replaced by a single mode ω_2. In the β form (space group $P6_222$, D_6^4, $Z = 3$) group theory yields:

$$\Gamma = 3A_1 + 5A_2 + 5B_1 + 5B_2 + 10E_1 + 8E_2$$

of which $1A_2 + 1E_1$ are acoustic modes. Only the A_1 and doubly degenerate E_1 and E_2 modes are Raman-active. The number of modes should thus decrease from 25 to 20 at the phase transition. In the present study, one mode was found to vanish at the phase transition. Based on polarization measurements, $4A_1$ features were observed in the β-quartz phase of $AlPO_4$ [6]. Although no polarization measurements were made for $Al_{0.80}Ga_{0.20}PO_4$, the same 4 A_1 features can be observed, along with, in the present case, the degenerate E_1 and E_2 modes. The presence of an additional mode, tentatively identified as the AlO_4 libration near 200 cm^{-1}, indicates that the above static, average high-symmetry model is not in agreement with the observed results. In the case of $AlPO_4$ [6], the additional A_1 mode was interpreted as evidence for dynamic disorder of the Al and P atoms over a set of lower-symmetry sites. Dynamic disorder has also been identified in β quartz by total neutron scattering [4].

The frequency of the E mode, initially at 107 cm^{-1}, decreases at a slower rate above the phase transition temperature of about 993 K (figure 3). The shift of this mode to lower frequency from room temperature up to the transition temperature is 20 cm^{-1}, which is relatively minor. No soft modes are observed and, instead, the librational modes of the tetrahedra, which are decoupled, have a strong tendency to become highly damped. Disorder appears to play a major role in the high-temperature behaviour of this material.

In previous work, the α–β phase transition temperature was linked to the frequency of the librational modes of the tetrahedral using a pseudo-spin Ising model [53]. It is difficult to reconcile this model to the presence of decoupled AlO_4 and GaO_4 modes rather than to one coupled mode. The α–β phase boundary in the x–T plane does not appear to be linked directly to the mode frequencies of these vibrations.

The β-quartz form was found to transform to the β-cristobalite form over a period of more than 90 min at 1073 K and almost immediately at 1173 K. The reverse transformations to either quartz forms were not observed upon annealing just below the phase transition temperatures or upon slow cooling. Instead, the transformation to the α-cristobalite form was observed at close to 500 K (figure 6). This behaviour is different to that of the gallium-rich samples. The average cation size is lower for the present composition, which will favour the less dense cristobalite

form and lowers the transition temperature. The transformations may be kinetically hindered at these lower temperatures. It was shown that, for $GaPO_4$, for example, the time required for the transition from β-cristobalite- to the α-quartz-type form increased from a few hours just below the phase transition temperature to a few days at 1123 K [27].

4. Conclusions

$GaPO_4$ and $Al_{1-x}Ga_xPO_4$ solid solutions were studied as a function of composition and temperature by Raman spectroscopy. Coupled and decoupled modes were identified in the spectra of the $Al_{1-x}Ga_xPO_4$ solid solutions. In particular, the tetrahedral tilting modes, which have been linked to high-temperature phase transitions to β-quartz-type forms, were found to be decoupled. The α–β quartz-type transition was only observed for the low-gallium-content $Al_{0.80}Ga_{0.20}PO_4$ sample and is associated with strong damping of the tetrahedral tilting modes. This damping can be linked to dynamic disorder. All samples transformed to the β-cristobalite form at high temperatures. The spectra of the high-temperature β-quartz and β-cristobalite forms are characterised by broad bands and additional modes with respect to the predictions of group theory for static ordered structures. These results are further evidence for the presence of a large degree of disorder in these phases. The reverse transition to the α-quartz form was found to occur the most readily for $GaPO_4$, followed by $Al_{0.62}Ga_{0.38}PO_4$. This may be related to the faster kinetics at the higher temperatures involved with respect to more Al-rich samples. In parallel, higher cooling rates were required to obtain the metastable α-cristobalite-type form in the samples with higher Ga-content.

References

[1] Heaney P J 1994 *Rev. Mineral.* **29** 1
[2] Keen D A and Dove M T 1999 *J. Phys.: Condens. Matter* **11** 9263
[3] Dove M T, Heine V and Hammonds K D 1995 *Mineral. Mag.* **59** 629
[4] Tucker M G, Keen D A and Dove M T 2001 *Mineral. Mag.* **65** 489
[5] Haines J, Cambon O, Keen D A, Tucker M G and Dove M T 2002 *Appl. Phys. Lett.* **81** 1
[6] Gregora I, Magneron N, Simon P, Luspin Y, Raimboux N and Philippot E 2003 *J. Phys.: Condens. Matter* **15** 4487
[7] Haines J, Cambon O, Prud'homme N, Fraysse G, Keen D A, Chapon L C and Tucker M G 2006 *Phys. Rev.* B **73** 014103
[8] Philippot E, Goiffon A, Ibanez A and Pintard M 1994 *J. Solid State Chem.* **110** 356
[9] Philippot E, Palmier D, Pintard M and Goiffon A 1996 *J. Solid State Chem.* **123** 1
[10] Philippot E, Armand P, Yot P, Cambon O, Goiffon A, McIntyre G J and Bordet P 1999 *J. Solid State Chem.* **146** 114
[11] Haines J, Chateau C, Léger J M and Marchand R 2001 *Ann. Chim. Sci. Mater.* **26** 209
[12] Haines J, Cambon O, Philippot E, Chapon L and Hull S 2002 *J. Solid State Chem.* **166** 434
[13] Haines J, Cambon O and Hull S 2003 *Z. Kristallogr.* **218** 193
[14] Cambon O, Yot P, Ruhl S, Haines J and Philippot E 2003 *Solid State Sci.* **5** 469
[15] Cambon O and Haines J 2003 *Proc. 2003 IEEE Int. Freq. Control Symp.—17th Eur. Freq. Time Forum* (Piscataway, NJ: IEEE) p 650
[16] Haines J, Cambon O, Astier R, Fertey P and Chateau C 2004 *Z. Kristallogr.* **219** 32
[17] Haines J and Cambon O 2004 *Z. Kristallogr.* **219** 314
[18] Cambon O, Haines J, Fraysse G, Detaint J, Capelle B and Van der Lee A 2005 *J. Appl. Phys.* **97** 074110
[19] Grimm H and Dorner B 1975 *J. Phys. Chem. Solids* **36** 407
[20] Raman C V and Nedungadi T M L 1940 *Nature* **145** 147
[21] Shapiro S M, O'Shea D C and Cummins H Z 1967 *Phys. Rev. Lett.* **19** 361
[22] Scott J F 1968 *Phys. Rev. Lett.* **21** 907
[23] Shigenari T, Imura Y and Takagi Y 1980 *J. Phys. Soc. Japan* B **49** (Suppl. B) 29
[24] Scott J F 1970 *Phys. Rev. Lett.* **24** 1107

[25] Scott J F 1974 *Rev. Mod. Phys.* **46** 83
[26] Shafer E C and Roy R 1956 *J. Am. Ceram. Soc.* **39** 330
[27] Perloff A 1956 *J. Am. Ceram. Soc.* **39** 83
[28] Barz R-U, Schneider J and Gille P 1999 *Z. Kristallogr.* **214** 845
[29] Jacobs K, Hofmann P, Klimm D, Reichow J and Schneider M 2000 *J. Solid State Chem.* **149** 180
[30] Miller W S, Dachille F, Shafer E C and Roy R 1963 *Am. Mineral.* **48** 1024
[31] Fursenko B A, Kirkinsky V A and Rjaposov A P 1980 *High-Pressure Science and Technology—Proc. 7th AIRAPT Int. Conf.* ed B Vodar and P Marteau (Oxford: Pergamon) p 562
[32] Balitsky V S, Balitsky D V, Nekrasov A N and Balitskaya L V 2005 *J. Physique* IV **126** 17
[33] Veksler I V, Thomas R and Wirth R 2003 *Am. Mineral.* **88** 1724
[34] Cachau-Herreillat D, Bennazha J, Goiffon A, Ibanez A and Philippot E 1992 *Eur. J. Solid State Inorg. Chem.* **29** 1295
[35] Xia H R, Qin Z K, Yuan W, Liu S F, Zou Z Q and Han J R 1997 *Cryst. Res. Technol.* **32** 783
[36] Xia H, Wang J, Li L and Zou Z 2000 *Prog. Cryst. Growth Charact. Mater.* **40** 253
[37] Barz R U, David F, Schneider J and Gille P 2001 *Z. Kristallogr.* **216** 501
[38] Haines J, Cambon O, Cachau-Herreillat D, Fraysse G and Mallassagne F E 2004 *Solid State Sci.* **6** 995
[39] Haines J, Cambon O, Fraysse G and Van der Lee A 2005 *J. Phys.: Condens. Matter* **17** 4463
[40] Mohamed F Sh 2002 *Adsorption Sci. Tech.* **20** 741
[41] Goullet A, Pascual J, Cusco R and Camassel J 1991 *Phys. Rev.* B **44** 9936
[42] Nakamura M, Orihara H, Ishibashi Y, Kim P and Hirano S 1990 *J. Phys. Soc. Japan* **59** 1831
[43] Ouillon R, Pinan-Lucarre J-P and Ranson P 2000 *J. Raman Spectrosc.* **31** 605
[44] Rokita M, Handke M and Mozgawa 2000 *J. Mol. Struct.* **555** 351
[45] Nicola J H, Scott J F and Ng H N 1978 *Phys. Rev.* B **18** 1972
[46] Dultz W, Quilichini M, Scott J F and Lehman G 1975 *Phys. Rev.* B **11** 1648
[47] Beaurain M, Armand P and Papet P 2005 *J. Cryst. Growth* **275** 279
[48] Beaurain M, Armand P and Papet P 2005 *J. Physique* IV **126** 23
[49] Shvanskii E, Armand P, Balitsky D, Philippot E and Papet P 2006 *Ann. Chim., Sci. Mater.* **31** 97
[50] Archary S N, Jayakumar O D, Tyagi A K and Kulshresththa S K 2003 *J. Solid State Chem.* **176** 37
[51] Worsch P, Koppelhuber-Bitschnau B, Mautner F A, Krempl P W and Wallnöfer W 1998 *Mater. Sci. Forum* **278–281** 600
[52] Haines J, Cambon O, Keen D A, Tucker M G and Chapon L C 2006 unpublished
[53] Engel G F and Krempl P W 1984 *Ferroelectrics* **54** 9